sisting of 50 mM tris (pH 8.0), 1% NP-40, 6 mM CHAPS, 150 mM NaCl, 5 mM EDTA, 0.5 mM Pefabloc SC (Boehringer Mannheim), and aprotinin (50 μg/ml; Sigma). Cell lysates were precleared with protein G–Sepharose (Sigma) and incubated with mAb 2F7 at a final concentration of 0.5 μg/ml for 6 hours at 4°C. Protein G–Sepharose was added to a final concentration of 1 μl/ml and immune complexes were allowed to form overnight at 4°C. Immune complexes were collected by centrifugation, and the pellets were washed 20 times with 1 ml of lysis buffer and resuspended in SDS-PAGE buffer containing dithiothreitol. After incubation at 100°C for 5 min, the supernatants were transferred to new tubes and kept at −20°C for further analysis. Standard SDS-PAGE was performed with 10% to 12.5% polyacrylamide gels. When required, proteins were silver-stained with the Silver Stain Plus system (Bio-Rad). For sequence determination, the mAb 2F7 ligand was immunoprecipitated from PAM cells (2×10^{10}), resolved by SDS-PAGE, and transferred to a polyvinylidene difluoride membrane (Millipore). The electroblotted 25-kD protein was excised after visualization with Amido black 10B (Bio-Rad). In situ digestion with trypsin was performed as described previously (*23*). Briefly, the excised band was treated with polyvinylpyrrolidone to prevent binding of the enzyme to the membrane. Digestion with trypsin {1 μg of 30 μl of 0.1 M TES [*N*-tris(hydroxymethyl)methyl-2-aminoethanesulfonic acid (pH 8.0)]} was allowed to proceed overnight. The supernatant was then fractionated by reversed-phase high-performance liquid chromatography. Fractions were collected manually based on absorbance at 210 nm. A fraction corresponding to a symmetrical peak was subjected to chemical sequence analysis on an ABI 470A protein sequencer (Applied Biosystems, Foster City, CA), and a unique sequence was obtained. The sequence was compared to other known protein sequences with the BLAST program (*24*).

28. Paraformaldehyde-fixed and polyester wax–embedded (*25*) day 14.5 whole embryo sections (10 μm) were hydrated in ethanol, soaked in 0.1 M citrate buffer (pH 6.0), and subjected to microwave treatment for 2 min on the highest setting (Radarange 1000W; Amana, IA). This treatment substantially improved the staining intensity obtained with mAb 2F7. The endogenous peroxidase activity was blocked, and the sections were incubated for 30 min in 2% FBS. The sections were then stained for 2 hours with biotinylated mAb 2F7, adjusted to 10 μg/ml in 1% FBS, and washed. Binding was visualized with streptavidin-labeled peroxidase (Jackson ImmunoResearch), followed by incubation in metal-enhanced diaminobenzidine (Pierce). No staining was observed when mAb 2F7 was omitted from the procedure. The sections were counterstained with hematoxylin, dehydrated in ethanol, cleared with Hemo-De (Fisher Scientific, Pittsburgh, PA), and mounted with DPX reagent (British drug house).
29. A complete murine CD81 complementary DNA (cDNA) was encoded by RT-PCR with oligonucleotide primers 5′-CGGAATTCATGGGGGTGGAGGGCTG-3′ and 5′-CGGAATTCTCAGTACACGGAGCTGTTC-3′. These primers were designed from the published murine CD81 gene sequence (*9*) and contained Eco RI restriction sites for cloning purposes. The complete CD81 cDNA was introduced into the eukaryotic expression plasmid pcDNA3 (Invitrogen) at the Eco RI site in the correct orientation for expression. We established stable CD81-expressing cells with Lipofectamine-mediated (Life Technologies) transfection of CHO-K1 cells followed by G418 selection. CD81 transfectants were selected by FACS after sequential incubations with biotinylated mAb 2F7 and fluorescein isothiocyanate (FITC)–streptavidin (Biomeda, Foster City, CA). Reaggregation cultures were performed as described (*5*). In brief, thymocytes (2×10^5) isolated from day 14.5 fetal thymus lobes were mixed with untransfected or CD81$^+$ CHO-K1 cells (1×10^5) centrifuged at 2000 rpm for 2 min in a microcentrifuge (Eppendorf), and the pellet resuspended in complete DMEM–10% FBS (4 μl). Before reaggregation, thymus cell preparations typically contained 98% CD25$^+$ cells and 2% CD81$^+$ cells, as evaluated by FACS analyses. Cells were deposited in 1-μl drops on the surface of polycarbonate filters supported with surgical Gelfoam (Upjohn) in complete DMEM–10% FBS (5 ml) and cultured for 5 days. After culture, cell pellets were disaggregated by resuspension in complete DMEM–10% FBS and stained with phycoerythrin antibody to CD4 (anti-CD4) and Red 613 antibody to CD8 before FACS analysis.
30. We thank S. Aaronson and L. Feng for providing cell lines; A. M. Gonzalez for advice and T. Wu for technical assistance with histochemistry; H. Shao for advice on reaggregation cultures; and J. Waters, J. Kaye, and J. Sprent for critical reading of the manuscript. Supported by a grant from the Lucille P. Markey Charitable Trust and by NIH grant AI32751 (W.L.H.). W.L.H. is a Lucille P. Markey Scholar and R.B. is a fellow of the Strohm Inflammatory Bowel Disease Center at the Scripps Clinic and Research Foundation. W.H.F. was supported in part by the Foundation for Medical Research, Inc. This is manuscript 9491-IMM from the Scripps Research Institute.

19 September 1995; accepted 9 November 1995

Effect of Polymorphism in the *Drosophila* Regulatory Gene *Ultrabithorax* on Homeotic Stability

Greg Gibson* and David S. Hogness

Development is buffered against unpredictable environmental and genetic effects. Here, a molecular genetic analysis of one type of developmental homeostasis, the establishment of thoracic segmental identity under the control of the *Ultrabithorax* (*Ubx*) gene in *Drosophila melanogaster*, is presented. Flies were artificially selected for differential sensitivity to the induction of bithorax phenocopies by ether vapor. The experiments demonstrated that increased sensitivity to ether correlated with a loss of expression of UBX in the third thoracic imaginal discs and that a significant proportion of the genetic variation for transcriptional stability can be attributed to polymorphism in the *Ubx* gene.

The specification of segmental identity in *Drosophila* depends on the coordination of complex expression patterns of homeotic genes in the Antennapedia and Bithorax complexes (*1*). This specification must also be a highly stabilized process, because morphological uniformity is produced despite environmental and genetic variation. However, as was shown by Gloor (*2*), the specification of segmental identity can nevertheless be disrupted by exposure of early embryos to ether vapor, which induces bithorax phenocopies that resemble homeotic transformations caused by mutations in the regulatory regions of the *Ubx* gene (*3*). Waddington later showed, by selecting populations that exhibit increased or decreased phenocopy frequencies, that genetic variation affects this process (*4*).

Starting with an outbred population of flies (*5*), we performed a selection experiment similar to that described by Waddington. The Ives strain is free from inversions and has been deliberately maintained with a high degree of heterozygosity (*6*). Embryos were collected at room temperature over a 1-hour period, and 2.5 hours later (that is, 3.0 ± 0.5 hours after eggs were laid) they were exposed to ether vapor for 10 min. More than 20 groups of about 400 embryos were treated each generation; upon emergence, the adults were scored for bithorax phenocopies. More than 1500 adults showing identity transformations of the third thoracic segment (T3), ranging from ectopic sternopleurae to near-complete replacement of halteres by wings (Fig. 1A), were selected for the next generation. Flies exhibiting such phenocopies were selected for eight generations. A steady increase in phenocopy frequency was observed in each generation (Fig. 2A, experiment 1), accumulating from 13% in the starting population to a plateau of 45%. Similar results were obtained in repetitions of the experiment 3 months later (Fig. 2A, experiment 2) and 2 years later (*7*). By contrast, the frequency of bithorax phenocopies dropped steadily when flies were selected for resistance to ether treatment (Fig. 2A, experiment 3) by breeding only from nontransformed flies. The results show that genetic variation exists for the propensity to exhibit ether-induced bithorax phenocopies in the Ives strain of *D. melanogaster* (*8*).

Several observations implicate the *Ubx* gene in the response to selection. (i) Many loss-of-function mutations in *Ubx* produce bithorax transformations similar to the ether-induced phenocopies (*9*). (ii) Flies heterozygous for mutations in genes that regulate the activation and maintenance of *Ubx* expression (including *hunchback* and *Polycomb*) exhibit altered bithorax phenocopy frequencies (*10*). (iii) Ether induced loss of UBX expression in patches within

G. Gibson, Department of Biology, University of Michigan, Ann Arbor, MI 48109–1048, USA.
D. S. Hogness, Department of Developmental Biology, Stanford University School of Medicine, Stanford, CA 94305–5427, USA.
*To whom correspondence should be addressed.

the imaginal discs that generate the segment (T3) affected by phenocopies (Fig. 1, B and C). After six generations of up-selection for phenocopies, ether induced this loss of UBX expression and the phenocopies at about the same frequency (*11*).

Our hypothesis is that the stability of a transcription complex that requires the regulatory regions in *Ubx* DNA for assembly can be affected by polymorphisms in these regions, or in the genes that encode the transcription factors, or both. Ether may further destabilize the complex beyond a threshold level, resulting in a loss of *Ubx* expression that is clonally propagated and causes spatially restricted bithorax transformations.

We screened for polymorphic sequences in randomly chosen 500–base pair stretches of *Ubx* DNA, as well as in several other candidate genes. A combination of polymerase chain reaction (PCR)–based DNA amplification from genomic DNA prepared from individual flies, single-strand conformation polymorphism (SSCP) (*12*), and heteroduplex analysis was used to detect polymorphisms resulting from substitution of one or several nucleotides. The locations of four polymorphisms are shown (Fig. 2C) (*13*, *14*). *Ubx* DNA (*3*) includes two large control regions (*15*), one upstream (UCR) and one downstream (DCR) of the transcription start site, that correlate, respectively, with the regions defined by the *bxd-pbx* and the *abx-bx* clusters of regulatory mutations (9). The *abdominal A* (*abdA*) gene is involved in the determination of abdominal segmental identities and has no known role in specifying the identity of T3 (*16*). Polymorphism D/d is in the 3′ untranslated trailer of *Ubx*, downstream of all documented regulatory regions of *Ubx* (*17*). Polymorphisms C/c and A/a lie at opposite ends of the UCR: C/c maps next to the *Ubx* promoter and A/a maps some 30 kb from it. Polymorphism Z/z is in the 5′ untranslated leader region of the *abdA* gene (*18*).

Pairwise linkage comparisons of these polymorphic markers were made from more than 100 chromosomes obtained from 72 flies of the Ives strain (Table 1). Significant linkage disequilibrium (D) at better than 90% power limits was observed among the markers within the *Ubx* gene, that is, for the AC, AD, Az, CD, and Cz pairs, for which the expression $D = f(XY) - f(X) \times f(Y)$ (where f is frequency) was significantly

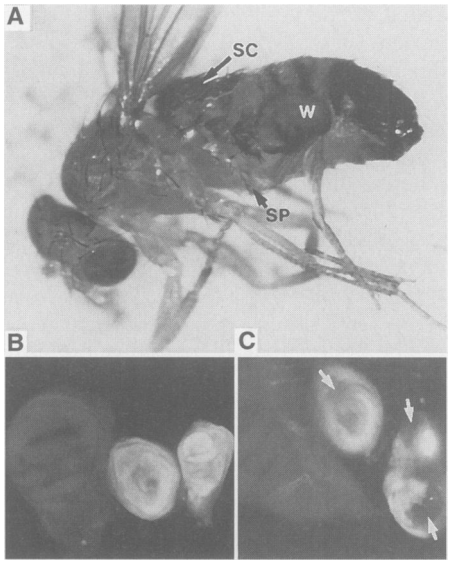

Fig. 1. Ether-induced phenotypes. (**A**) Photograph of a fly with an extreme bithorax phenocopy, showing near-complete duplication of the dorsal mesothorax. The extra wing (W) is uninflated, possibly because of an improper connection to the trachea. SP, sternopleural bristles, characteristic of T2 legs; SC, scutellum. (**B** and **C**) Immunohistochemical staining of UBX protein in third-instar haltere imaginal discs dissected from larvae with (C) and without (B) a 10-min exposure to ether at the cellular blastoderm stage. Arrows show patches in which UBX expression has been lost. Monoclonal antibody FP3.38 was provided by D. Brower, with rhodamine-labeled secondary antibody (Jackson Laboratory) used as previously described (*15*).

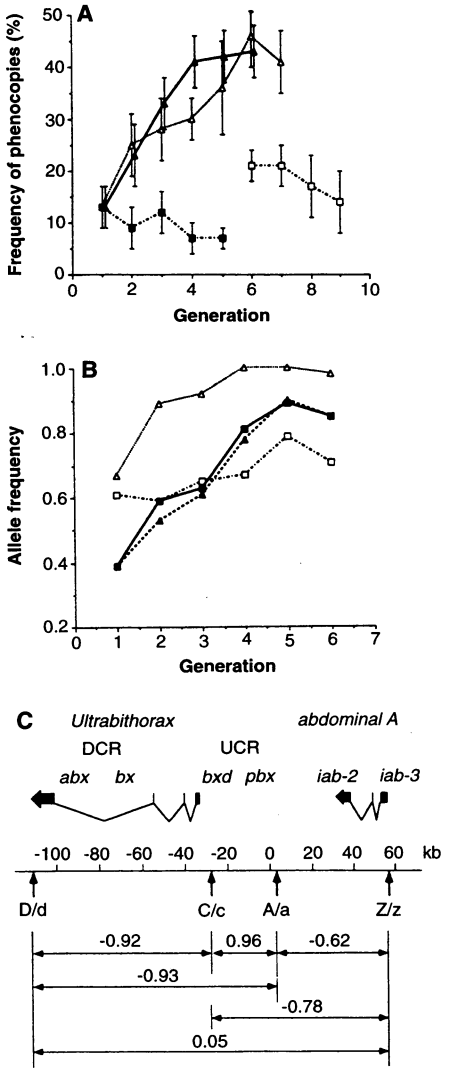

Fig. 2. Responses to selection. (**A**) Frequencies of bithorax phenocopies observed in each generation. Error bars show one standard deviation unit around the mean of up to 20 individual treatments. Experiment 1 (△) and experiment 2 (▲) involved selection for increased propensity to phenocopy. In experiment 3 (■), selection was for resistance to ether; because of the low percentages and relatively weak response, the length of ether treatment was increased from 10 to 12 min after the fifth generation (□). (**B**) Allele frequency shifts in response to up-selection in experiment 2. Allele A, ■; allele C, ▲; allele D, △; allele z, □. Most points are ±5%. (**C**) Location of polymorphisms. The extents of the *Ubx* and *abdA* transcripts are shown above a line measuring distances in kilobases along the molecular map of the cloned region (*3*). Exons are indicated by black boxes, with the direction of transcription shown. Proximal (toward the centromere) is to the left. The ratio D/D_{max} (that is, D' from Table 1) is shown for each polymorphism pair below the map.

Table 1. Disequilibrium statistics for the Ives strain. For each of the first five pairwise comparisons, AC, AD, Az, CD, and Cz, the χ^2 value implies $P < 0.01$, and the null hypothesis that $D = 0$ can be rejected. Two further statistics confirm that the observed linkage disequilibrium is real (*19*): In each case, $n > n_{min}$ indicates that more gametes were examined than would be required to reject the null hypothesis with 95% probability for the observed allele frequencies and value of D; and $|D| > D_{min}$ similarly indicates that the value of D is greater than that required to reject $D = 0$ for the given sample size. By contrast, the two flanking markers D and z have $P > 0.8$ for the χ^2 value with 1 degree of freedom, and there is no basis for rejecting the hypothesis that they are in linkage equilibrium. Results are shown for estimates of haplotype frequencies when double heterozygotes were excluded, but statistically similar conclusions were obtained when these were included in the analysis. The genetic distance from C to D is ~0.7 centimorgans (*21*). $D = f(XY) - pu$, where $p = f(X)$ and $u = f(Y)$. $D' = D/D_{max}$. $D_{max} = \min [p(1 - u); (1 - p)u]$ if $D > 0$ or $\min[pu; (1 - p)(1 - u)]$ if $D < 0$. n = number of gametes scored; $n_{min} = [10.51\ p(1 - p)u\ (1 - u)]/D^2$; $\chi^2 = nD^2/p\ (1 - p)u(1 - u)$; $D_{min} = \sqrt{[10.51\ p(1 - p)u(1 - u)/n]}$.

Pairwise comparison	n (n_{min})	D	D_{max}	D'	χ^2	D_{min}
AC	118 (12)	0.222	0.232	0.96	104	0.071
AD	126 (37)	−0.122	0.132	−0.93	35	0.067
Az	118 (61)	−0.100	0.160	−0.62	20	0.071
CD	108 (36)	−0.126	0.136	−0.92	36	0.072
Cz	104 (50)	−0.107	0.137	−0.78	22	0.074
Dz	110 (na)	0.005	0.115	0.05	0.06	0.069

different from zero (*19*). In contrast, D and z, the two markers that flank the 170-kb region that includes *Ubx* and part of *abdA* (Fig. 2C), appeared to associate randomly. Because linkage disequilibrium in *Drosophila* has been observed to decay over just 2 kb (*20*), its persistence over 110 kb [about 0.1 centimorgans (*21*)] for the AD pair is notable, although similar levels have been documented within the *achaete-scute* complex and *Ddc* (*22*). Linkage in the case of the present experiment is a property of the starting population, and recombination is not expected to have a significant effect on the observed associations between alleles at intermediate frequencies in the time course of this experiment.

Changes in frequency of the four *Ubx* alleles in response to selection during the second of the up-selection experiments are plotted (Fig. 2B). Similar responses were obtained in all repetitions. The frequencies of alleles at the end points of both experiments, when the phenocopy frequency was between 41 and 45%, are shown (Table 2). Whereas allele D was close to fixation at this point, the tightly linked alleles A and C showed greater overall increases in frequency (0.45 to 0.48 as compared with 0.31 to 0.33 for D) and allele z showed a relatively weak, though replicated, increase.

The finding that all four polymorphisms examined showed changes in frequency and the observation that the two flanking markers (D and z) were in linkage equilibrium imply that at least one selectable polymorphism lies within this region of the Bithorax complex. Selection focused adjacent but external to one of these markers would not be expected to affect the frequency of the other marker. Although it is possible that multiple polymorphisms in the region are being selected, the data are consistent with there being a single selected site within *Ubx*. This consistency is exemplified by the agreement between the observed frequencies and the predicted final frequencies of the C, D, and z alleles if selection is assumed to act on A, given the starting associations among alleles (Table 2).

The simplest interpretation of the data places the selected site or sites in the DCR of *Ubx*. This conclusion assumes, as supported by the data, that linkage disequilibrium decreases with distance along the chromosome. It remains possible that the selected site lies elsewhere in the genome but happens to show extreme linkage disequilibrium with the *Ubx* polymorphisms. This could occur by chance for a rare allele, but it is unlikely that such associations would be maintained over several years in two large populations of the same strain. Furthermore, the selected allele must be at an initial frequency greater than 0.1 to account for the selection response, given any reasonable selection coefficients. Alternatively, linkage disequilibrium could be maintained by epistatic interactions with another closely linked locus. Given the absence of any other strong candidate loci in the region, this seems less likely, and if true would imply further that polymorphisms in *Ubx* are exposed to selection in the base population.

Three further sets of observations strengthen the inference that a functionally distinct polymorphism exists within the *Ubx* gene. (i) The frequencies of three other polymorphisms in distinct loci at different chromosomal locations remained constant throughout the course of the experiments (Table 3) (*23*). (ii) The shifts in frequency of the four BX-C alleles (A, C, D, and z) in response to selection for resistance to ether in the down-selection experiment were, as expected, in the opposite direction and were in proportion to the magnitude of effects for increased sensitivity to ether (Table 2, experiment 3). (iii) A significant correlation between bithorax phenocopy frequency and *Ubx* genotype was seen in the progeny of pair matings of flies taken at random from the unselected Ives strain (*24*).

The *Ubx* polymorphism is not the only source of genetic variation affecting sensitivity to ether, but it clearly has a major effect (*24*). One or more trans-acting loci are likely to have a maternal effect (*4*) because there is a significant difference between phenocopy frequencies in the F_1 generations of reciprocal crosses (*25*). Several genes that regulate *Ubx* transcription are expressed maternally (*1*) and these may be regarded as candidate modifier loci. Our results provide further evidence that polymorphisms in regulatory genes that encode transcription factors can contribute genetic variation for morphological traits (*26*). Understanding how genetic variation is maintained in complex epistatic and pleiotropic developmental pathways (*27*), especially in the context of a phenotypically uniform but genetically variable trait, will help to clarify the mechanistic basis of both developmental homeostasis and evolutionary canalization.

Table 2. Summary of changes in allele frequencies. The allele frequencies (Freq.) of A, C, D, and z for *n* chromosomes in five populations are shown: Ives, after seven generations of selection in experiment 1, after five generations of selection in experiment 2, after nine generations of selection for resistance to ether in experiment 3, and after six generations of selection in experiment 4. Genotype frequencies in the starting strains were virtually identical (A = 0.39; C = 0.38; *n* = 96 for the Michigan population). Δ indicates the change in frequency with respect to Ives. Exp. is the expected frequency if the A allele were the sole focus of selection, calculated by reference to nonrandom associations between alleles in the Ives strain. There was no significant difference between these expected values and the observed frequencies ($P > 0.6$ for experiments 1 to 3, χ^2 test). ND, not determined.

Allele	Freq.	*n*	Δ	Exp.
		Ives		
A	0.39	140	—	—
C	0.39	122	—	—
D	0.67	128	—	—
z	0.61	122	—	—
		Experiment 1		
A	0.87	68	0.48	0.87
C	0.84	62	0.45	0.86
D	1.00	62	0.33	0.91
z	0.81	72	0.20	0.78
		Experiment 2		
A	0.85	68	0.46	0.85
C	0.85	60	0.46	0.83
D	0.98	68	0.31	0.90
z	0.71	62	0.10	0.78
		Experiment 3		
A	0.11	72	−0.28	0.11
C	0.13	72	−0.26	0.13
D	0.58	72	−0.09	0.53
z	0.52	52	−0.09	0.46
		Experiment 4		
A	0.89	120	0.50	0.89
C	0.88	120	0.50	0.85
D	ND	ND	ND	ND
z	ND	ND	ND	ND

Table 3. Frequencies of control polymorphisms. Markers at three different chromosomal locations (*bcd*, 3-[47.5], 84A; *EcR*, 2-[55.2], 42A; *GS1*, 2-[0.1], 21B) had insignificant linkage disequilibrium with the *Ubx*-A marker at 3-[58.8], 89E. At the conclusion of experiment 1, the frequencies of each of these markers were within one standard deviation unit of the frequency in the Ives starting population, calculated as the binomial variance of frequencies. See Table 1 for symbol definitions.

Polymorphism	Ives strain	Experiment 1	*D'* with A	χ^2	*P*
bicoid	0.48 ± 0.04	0.44	0.064	0.33	>0.6
EcR	0.63 ± 0.06	0.66	0.075	0.31	>0.6
GS1	0.75 ± 0.04	0.73	0.076	0.18	>0.7

REFERENCES AND NOTES

1. G. Morata, *Curr. Opin. Genet. Dev.* **3**, 606 (1993).
2. H. Gloor, *Rev. Suisse Zool.* **54**, 637 (1947).
3. W. Bender *et al.*, *Science* **221**, 23 (1983); D. S. Hogness *et al.*, *Cold Spring Harbor Symp. Quant. Biol.* **50**, 181 (1985).
4. C. H. Waddington, *Evolution* **10**, 1 (1956).
5. More than 1500 flies per generation were maintained in cages at room temperature (23°C) and fed standard yeasted cornmeal. From 5 to 10 collections of 1 hour each were made per day; embryos were allowed to age for 2.5 hours at 23°C, then washed onto a small sieve and transferred to an agar plate. The plate was inverted over a wad of ether-saturated cotton wool in

a milk bottle for 10 or 12 min. The plate was then placed in a bottle containing yeasted cornmeal; emerging adults were scored and selected 10 days later.
6. B. Charlesworth and D. Charlesworth, *Heredity* **54**, 71 (1985). The Ives strain was initially isolated in Massachusetts more than 20 years ago and was put through a bottleneck of 50 pair matings, which removed any segregating, cytologically visible inversions.
7. The first two experiments at Stanford were performed with flies obtained from G. Spicer. These flies were established from B. Charlesworth's stock, which was used for the later repetition at Michigan. The stocks used have been isolated for at least 4 years, and both have been maintained by ordered rotation of 10 bottles each generation.
8. The heritability (h^2) of phenocopy liability can be estimated by following Falconer's method for threshold-dependent traits [D. S. Falconer, *Introduction to Quantitative Genetics* (Longman, New York, ed. 2, 1981), p. 272]: $h^2 = (x_P - x_R)/i$ where x_P and x_R are the proportions of phenocopied individuals in the parental (Ives) and progeny populations, respectively, and i is the intensity of selection, all expressed in standard deviation units. For percentages of 13 and 24% (the mean frequencies in the F_1 generation of the three selection experiments) the values were as follows: $x_P = 1.126$, $x_R = 0.706$, $i = 1.627$, and $h^2 = 0.26$. However, the error associated with the measurements was high: The ratio of genetic to phenotypic variance was in the range of 0.15 to 0.40, if an underlying normal distribution of threshold-dependent liability is assumed.
9. E. B. Lewis, *Nature* **276**, 565 (1978); I. Duncan, *Annu. Rev. Genet.* **21**, 285 (1987).
10. M. P. Capdevila and A. García-Bellido, *Wilhelm Roux's Arch. Dev. Biol.* **190**, 339 (1981).
11. Five of 17 sets of discs from larvae treated after six generations of up-selection showed patches of lost expression. This finding is in agreement with the frequency of phenocopies seen in these animals. Zero of 12 sets of discs from animals not treated with ether showed loss of UBX expression.
12. E. P. H. Yap and J. O. McGee, *Trends Genet.* **8**, 49 (1992).
13. In addition to the four Bithorax complex polymorphisms discussed in the text, two sequences sampled from the coding region appeared to be monomorphic, one sequence from the *bxd* region amplified inconsistently, and a fifth polymorphism in the *pbx* region within 5 kb of A/a gave genotype values almost identical to A/a.
14. The primer locations are contained in the complete sequence of the Bithorax complex (GenBank accession number U31961). Primer pairs for PCR amplification were as follows: A/a, ACATGAAAACATTTGCGTAA and TTATGCGCCGTCGCTCTAAA; C/c, ACGTTGCATTTGCCGTTGCA and AGAAGGGGTGGTGCA (originally from unpublished *Ubx* sequence, D. Peattie and D. S. Hogness); D/d, TTGAGAGAGTCTTCGCG and GGTATCGGTATGGTATCGG [nt 3226 to 3362 of (*17*)]; and Z/z, GCACCACCCACAGGTGCA and TTGCTCGCATTCAACATT [nt 257 to 745 of (*18*)]. PCR reactions were carried out in an Ericomp or Perkin-Elmer machine, with 40 cycles. Each cycle consisted of 30 min at 94°C, 30 min at 57°C, and 45 min at 72°C and was started with about 50 ng of genomic DNA prepared from a single fly, in 25-μl reactions at 1 mM Mg. For alleles A and C, 10 μl of product was run directly into a 6.5% polyacrylamide gel in 1 × TAE (0.04 M tris and 1 mM EDTA adjusted to pH 7.4 with acetate) maintained at 25°C; polymorphisms were detected as heteroduplexes. Samples of alleles D and Z (9 μl) were first denatured with 1 μl of 0.1 M NaOH and 5 mM EDTA for 5 min at 37°C and then with 1 μl of formamide before they were loaded. Samples of allele Z were also digested before denaturation with Pvu II restriction enzyme to create products small enough to resolve by SSCP (*12*). Bands were detected by ethidium bromide staining or by radiography after inclusion of a trace amount of ^{35}S-labeled dATP in the PCR reactions.
15. K. D. Irvine, S. Helfand, D. S. Hogness, *Development* **111**, 407 (1991); J. Simon, M. Peifer, W. Bender, M. O'Connor, *EMBO J.* **9**, 3945 (1990).
16. A. Busturia, J. Casanova, E. Sanchez-Herrero, R. Gonzales, G. Morata, *Development* **107**, 575 (1989).
17. K. Kornfeld *et al.*, *Genes Dev.* **3**, 243 (1989).
18. F. Karch, W. Bender, B. Weiffenbach, *ibid.* **4**, 1573 (1990).
19. C. Zapata and G. Alvarez, *Evolution* **46**, 1900 (1992).
20. J. N. Macpherson, B. S. Weir, A. J. Leigh Brown, *Genetics* **126**, 121 (1990).
21. M. E. Akam, H. Moore, A. Cox, *Nature* **309**, 635 (1983).
22. C. F. Aquadro *et al.*, *Genetics* **132**, 443 (1992); W. G. Hill and A. Robertson, *Theor. Appl. Genet.* **38**, 226 (1968).
23. *GS1*: R. Caizzi, M. P. Bozzetti, C. Caggese, F. Ritossa, *J. Mol. Biol.* **212**, 17 (1990); *EcR*: M. R. Koelle *et al.*, *Cell* **67**, 59 (1991); *bicoid*: T. Berleth *et al.*, *EMBO J.* **7**, 1749 (1988).
24. The contribution of the major *Ubx* polymorphism to the genetic variance can be estimated from the relation $h^2 = 2pq[a + (q - p)d]/s^2$ where a and d are the additive and dominance effects associated with the polymorphism. Estimates based on determination of the mean frequencies of 15 isofemale lines that are homozygous or heterozygous for either the A or a alleles yield values of $a = 11.8$ and $d = -6.8$ (G. Gibson, unpublished data) against a total standard deviation of 16.0 percentage units. For $p = 0.39$ in the Ives strain, h^2 due to *Ubx* was 0.196. The arcsin ($\sqrt{x}$) transformed data yield an estimate of 0.170. If the departure from additivity due to recessivity is ignored, this estimate suggests that a polymorphism linked to *Ubx*-A would contribute between 65 and 75% of the genetic variance, given the overall heritability estimate in (*8*). However, given the error associated with all measurements and uncertainties about the additivity or normality, or both, of the underlying liability distribution, the estimate has very low confidence. Better estimates await identification of the remaining liability-effect loci.
25. Resistant (or sensitive) virgin females were crossed en masse to sensitive (or resistant) males, and phenocopy frequencies were determined from multiple trials. Significant results were obtained with stocks at the conclusion of both the second Stanford experiment (20% compared with 5%, 10-min ether treatments; $P < 0.005$, $n = 5$ trials, t test) and the Michigan experiment [35% compared with 25%, 15-min ether treatments; $P < 0.02$, $n = 6$; the parents in this case were from isofemale lines and showed extreme sensitivity (55%) and resistance (2%), respectively]. Comparison of males and females independently yielded identical conclusions, indicating that there was no strong contribution from the X chromosome.
26. C. Lai, R. F. Lyman, A. D. Long, C. H. Langley, T. F. C. Mackay, *Science* **266**, 1697 (1994); T. F. C. Mackay and C. H. Langley, *Nature* **348**, 64 (1990); S. Tanksley, *Annu. Rev. Genet.* **27**, 205 (1993).
27. L. A. Zhivotovsky and S. Gavrilets, *Theor. Popul. Biol.* **42**, 254 (1992).
28. We thank B. Charlesworth and G. Spicer for supplying us with the Ives strains, M. Bender for assistance in the early stages, and R. Fuller and C. Goodnow for the use of their PCR machines. G.G. particularly thanks W. Watt, M. Feldman, and J. Adams for their support and advice and D. Pollock, M. Montano, D. Andrew, and members of the Feldman and Hogness laboratories for comments and discussions. Supported by grants from the Rackham Graduate School of the University of Michigan and by grants to D.S.H. from the National Institutes of Health. G.G. was supported by a postdoctoral fellowship from the Helen Hay Whitney Foundation.

14 August 1995; accepted 24 October 1995

Structure of the Heat Shock Protein Chaperonin-10 of *Mycobacterium leprae*

Shekhar C. Mande, Vijay Mehra, Barry R. Bloom, Wim G. J. Hol*

Members of the chaperonin-10 (cpn10) protein family, also called heat shock protein 10 and in *Escherichia coli* GroES, play an important role in ensuring the proper folding of many proteins. The crystal structure of the *Mycobacterium leprae* cpn10 (Ml-cpn10) oligomer has been elucidated at a resolution of 3.5 angstroms. The architecture of the Ml-cpn10 heptamer resembles a dome with an oculus in its roof. The inner surface of the dome is hydrophilic and highly charged. A flexible region, known to interact with cpn60, extends from the lower rim of the dome. With the structure of a cpn10 heptamer now revealed and the structure of the *E. coli* GroEL previously known, models of cpn10:cpn60 and GroEL:GroES complexes are proposed.

Mycobacteria are among the most important human microbial pathogens. *Mycobacterium tuberculosis* is estimated to be responsible for 2.02 million deaths per year, particularly in developing countries, and has recently reemerged in the industrialized countries (*1–3*). *Mycobacterium leprae* causes a disfiguring disease, leprosy, in 30% of the untreated cases. Mycobacteria have many unusual features, one of the most remarkable being the ability of these organisms to reside in Schwann cells and macrophages, the latter being the very cells that should destroy the invading organisms. One of the important antigens of *M. leprae* recognized by T cells is cpn10, a 10-kD heat shock protein. In patients with tuberculoid leprosy, approximately one-third of the *M. leprae*–reactive T cells that respond to the whole organism also respond to cpn10 (*4*). We report here the crystal structure of *M. leprae* cpn10 (Ml-cpn10).

Members of the cpn10 family, GroES in

S. C. Mande, Department of Biological Structure and Biomolecular Structure Center, University of Washington, Seattle, WA 98195, USA.
V. Mehra, Department of Microbiology and Immunology, University of Washington, Seattle, WA 98195, USA.
B. R. Bloom, Department of Microbiology and Immunology, University of Washington, Seattle, WA 98195, USA, and Howard Hughes Medical Institute, Albert Einstein College of Medicine, Bronx, NY 10461, USA.
W. G. J. Hol, Department of Biological Structure and Biomolecular Structure Center, and Howard Hughes Medical Institute, University of Washington, Box 357742, Seattle, WA 98195, USA. E-mail: hol@xray.bmsc.washington.edu

*To whom correspondence should be addressed.